Electronic Supplementary Material (ESI) for RSC Advances.

Electronic Supplementary Information (ESI†)

Cetyl Alcohol Mediated Synthesis of $CuCr_2O_4$ Spinel Nanoparticles: A Green Catalyst for Selective Oxidation of Aromatic C-H Bonds with Hydrogen Peroxide

Shankha S. Acharyya,[a] Shilpi Ghosh,[a] Nazia Siddiqui,[a] L.N. Sivakumar Konathala,[a] and Rajaram Bal*[a]

[a] *Catalytic Conversion & Processes Division, CSIR-Indian Institute of Petroleum, Dehradun-248005, India*

Corresponding author. Tel.: +91 135 2525917; Fax: +91 135 2660202

E-mail addresses: raja@iip.res.in

Detailed Characterization Techniques:

1. X-ray power diffraction (XRD)

Powder X-ray diffraction patterns were collected on a Bruker D8 advance X-ray diffractometer fitted with a Lynx eye high-speed strip detector and a Cu K_α radiation sourceusing Cu Ka radiation with a wavelength of 1.5418 Å. Diffraction patterns in the 2°-80°region were recorded at a rate of 0.5 degrees (2θ) per minute. The resulting XRD profiles were analyzed to identify the crystal phase of the compound using reference standards. The line width of the most intense XRD peak was taken for estimation of crystallite size by the Scherrer equation.

2. Scanning electron microscopy (SEM)

Scanning electron microscopy images were taken on a FEI Quanta 200 F, using tungsten filament doped with lanthanumhexaboride (LaB_6) as an x-ray source, fitted with an ETD detector with high vacuum mode using secondary electrons and an acceleration tension of 10 or 30 kV. Samples were analyzed by spreading them on a carbon tape. Energy dispersive X-ray spectroscopy (EDX) was used in connection with SEM for the elemental analysis. The elemental mapping was also collected with the same spectrophotometer. Samples were subjected to scanning electron microscope analysis to understand the shape, size, and morphology properties.

3. Transmission electron microscopy (TEM)

The particle size and distribution of the samples were analyzed by TEM, JEOL JEM 2100 microscope, and samples were prepared by mounting an ethanol-dispersed sample on a lacey carbon Formvar coated Cu grid.

4. X-ray photoelectron spectroscopy (XPS)

X-Ray photoelectron spectra were recorded on a Thermo Scientific K-Alpha X-Ray photoelectron spectrometer and binding energies (±0.1 eV) were determined. The resulting spectra were analyzed to identify the different oxidation states of the copper and chromium ions present in the sample. Prior to the analysis, the spectra were calibrated with reference to C1s observed at a binding energy of 284.5 eV.

5. Inductively coupled Atomic Absorption Spectroscopy (ICP-AES)

Chemical analyses of the metallic constituents were carried out by Inductively Coupled Plasma Atomic Emission Spectrometer; model: PS 3000 uv, (DRE), Leeman Labs, Inc, (USA).

6. Thermogravimetric Analyses (TGA) of the uncalcined catalyst were carried out in a Pyris Diamond, Perkin Elmer Instruments, and Technology by SII (Seiko Instruments INC), USA] instrument-balance by heating 2.15 mg samples at 5 $^{\circ}$C min^{-1} in flowing air atmosphere.

Experimental

Materials

Hydrogen Peroxide (50 wt % in water) was purchased from Merck KGaA, Darmstadt, Germany. $Cu(NO_3)_2 \cdot 5H_2O$, $Cr(NO_3)_3 \cdot 9H_2O$, cetyl alcohol, hydrazine, ammonium hydroxide, benzene (purity > 99.9%), acetonitrile (HPLC grade) were purchased from Sigma-Aldrich Co. All the chemicals were used without further purification.

Detailed Experimental Procedure

Catalyst Preparation: The $CuCr_2O_4$ spinel nanoparticles were prepared hydrothermally by modifying our own preparation method taking nitrate precursors of copper and chromium. All chemicals were used without further purification. All solvents used were of reagent grade. All syntheses were carried out under ambient conditions. In a typical synthesis procedure, an aqueous solution of 2.7 g $Cu(NO_3)_2.3H_2O$ (from Sigma Aldrich) was added with vigorous stirring to 9.0 g $Cr(NO_3)_3.9H_2O$ (from Sigma Aldrich) dissolved in 47 g deionized water (mixed with 12g pure ethanol) to give a clear dark blue homogeneous solution. By gradual addition of few drop ammonia solution, the pH of the solution was made 8. Hot solution of 2.0 g cetyl alcohol (from Sigma Aldrich) was added dropwise followed by addition of 0.72 g hydrazine (from Sigma Aldrich) to the reaction mixture. The reagents were added maintaining the molar ratio of Cu: Cr: CTAB: H_2O: hydrazine = 1: 2: 0.75: 250: 1. After stirring, the so obtained homogeneous solution was hydrothermally treated at 180 °C for 24 h in a Teflon-lined autoclave vessel under autogeneous pressure. After the required period, the autoclave was allowed to cool at room temperature. Then, the solid product was collected by means of centrifugation at 18,000 rpm and dried at 120 °C, for 10 h, followed by calcination at 750 °C for 6 h in air (ramped at 1° C/min) to get $CuCr_2O_4$ spinel nanoparticles.

Liquid phase hydroxylation

Liquid phase oxidation reaction was carried out in a two neck round bottom flask, equipped with refrigerant, containing 0.05 g catalyst, 10 ml solvent and 1 g benzene to which H_2O_2 (50% aq. solution) was added dropwise to prevent immediate H_2O_2 decomposition. The flask was then emerged in a preheated oil bath and vigorously stirred with a magnetic stirrer. All experiments were carried out at 75 °C.Small aliquots of the sample were withdrawn from the reaction mixture at regular intervals for analysis using a syringe. At the end of the reaction, the solid particles (catalyst) were separated by filtration and the products were analysed by Gas Chromatograph (GC, Agilent 7890) connected with a HP5 capillary column (30m length, 0.28 mm id, 0.25 μm film thickness) and flame ionisation detector (FID). Chem Station software was used to collect and analyze the respective GC-data. The relative error of product determination did not exceed ±5%. The benzene conversion and phenol formation were calculated using a calibration curve (obtained by manual injecting the authentic standard compounds). An anisole solution with a known amount was used as an external standard for analysis. The individual yields were calculated and normalized with respect to the GC response factors. The product identification was carried out by injecting the authentic standard samples in GC and GC-MS. The product was separated from the reaction mixture by means of column chromatography and was further confirmed by ^{1}H NMR. For the reusability test, the catalyst was repeatedly washed with acetonitrile and acetone and dried overnight at 110 °C and used as such, without regeneration. In order to check the metal leaching the mother liqor was then analyzed using ICP-AES.

Material Balance

We have performed the C-balance as well as material balance for few experiments. The estimated error in analysis arising due to sampling and handling losses was $\pm$ 5%.

XPS: The Cu2p spectrum of the fresh sample is characterized by two spin orbit doublets with strong satellite peaks. The so obtained Cu2p$_{3/2}$ signals fitted satisfactorily to two principal peak components at ~ 935.2 and 933.8 eV. The BE for the Cu2p peak was in close agreement with that of $CuCr_2O_4$ indicating that, the main phase is $CuCr_2O_4$ spinel. The low energy component with Cu2p$_{3/2}$ at 933.8 eV is associated to Cu^{2+} in octahedral sites, whereas the high component at 935.2 eV is associated to Cu^{2+} in tetrahedral sites. The Cr$_{2p\ 3/2}$ core level spectra of the $CuCr_2O_4$ fresh catalyst appeared at 576.6 eV which shows the presence of Cr^{3+} ions in $CuCr_2O_4$ spinel and the O_{1s} binding energies appeared at 530.2 eV and 532.2 eV, revealed the presence of O^{2-} species in $CuCr_2O_4$ spinel.[1-3]

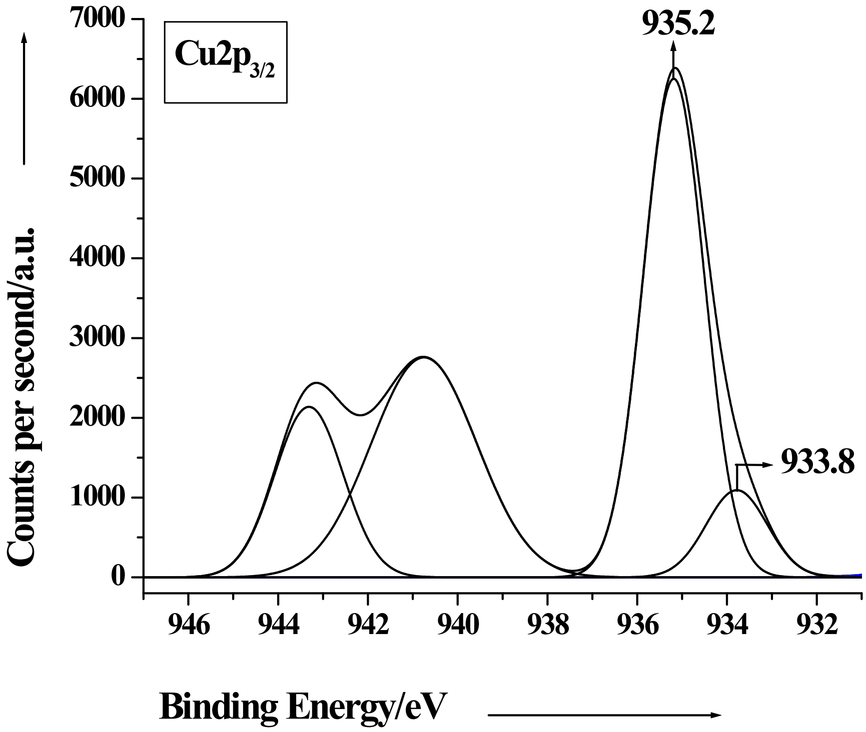

Fig. S1 Cu 2p$_{3/2}$ core level spectra of the catalyst.

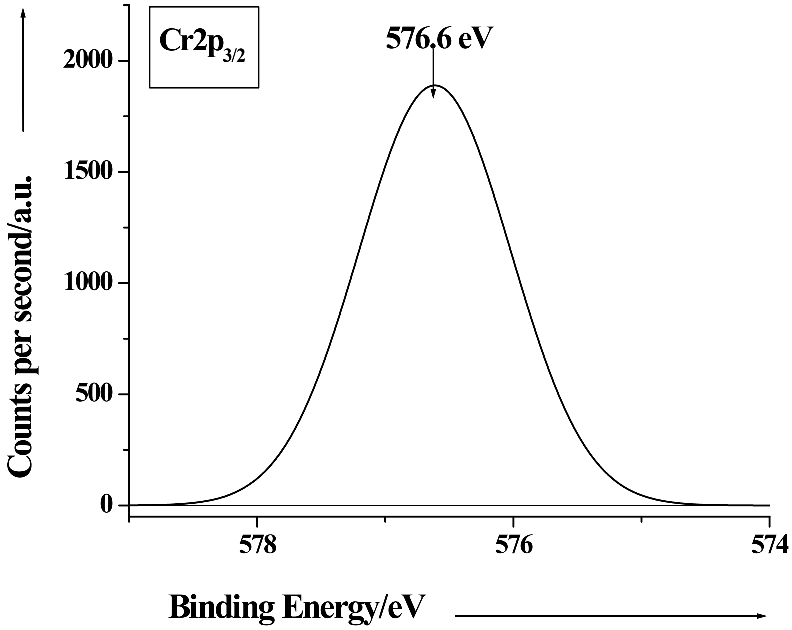

Fig. S2 Cr 2p$_{3/2}$ core level spectra of the catalyst.

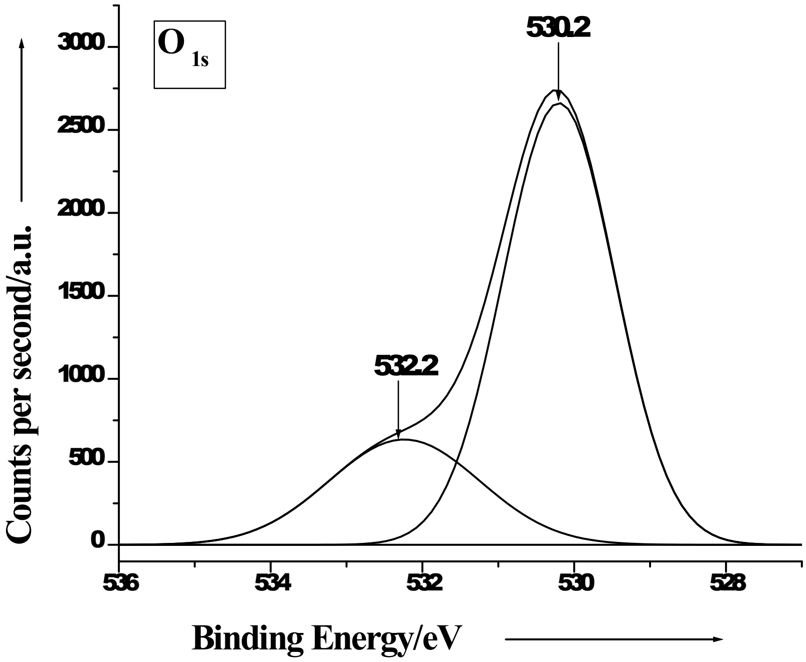

Fig. S3 O$_{1s}$ core level spectra of the catalyst.

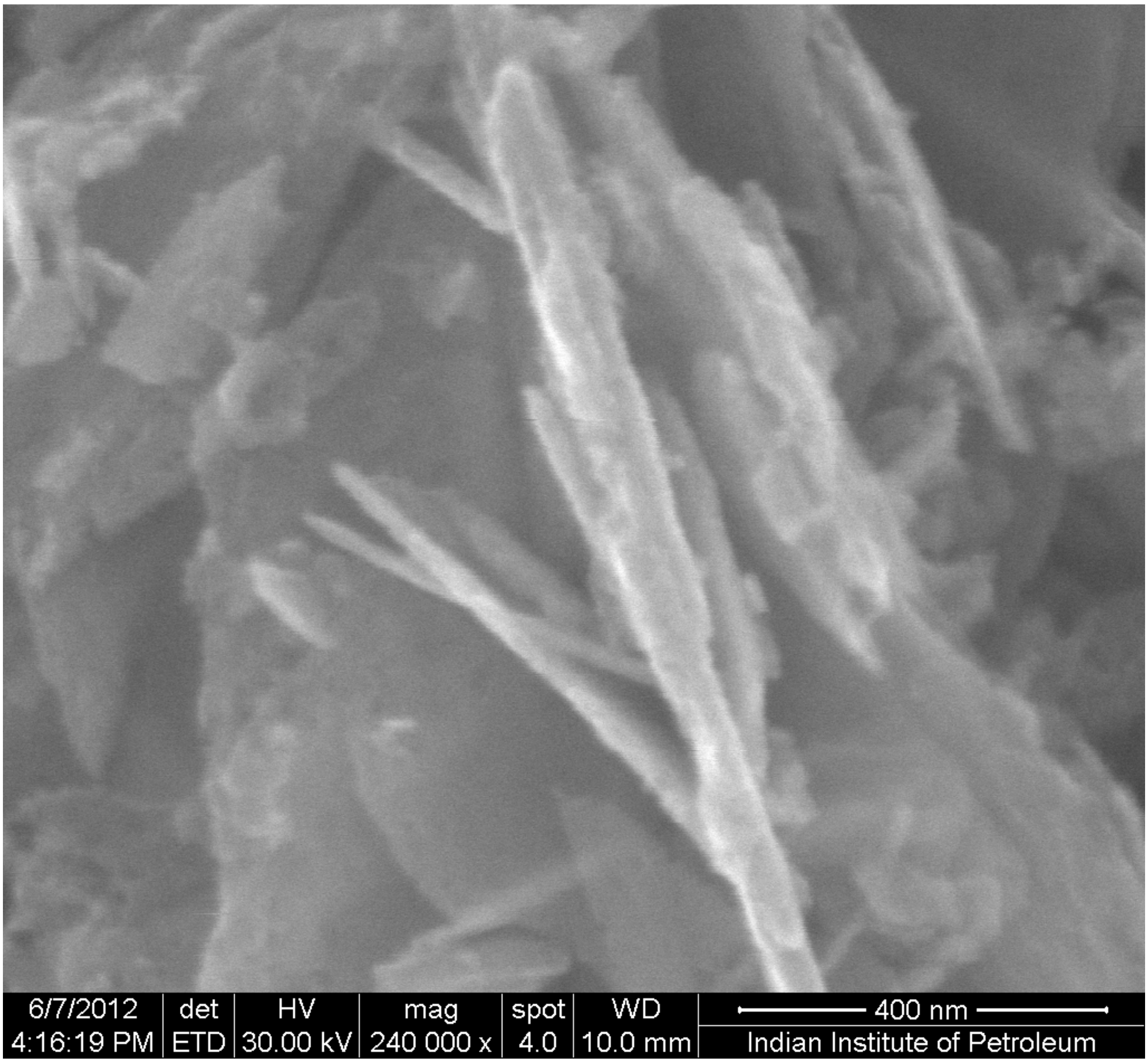

Fig. S4 SEM image of commercial $CuCr_2O_4$ spinel catalyst.

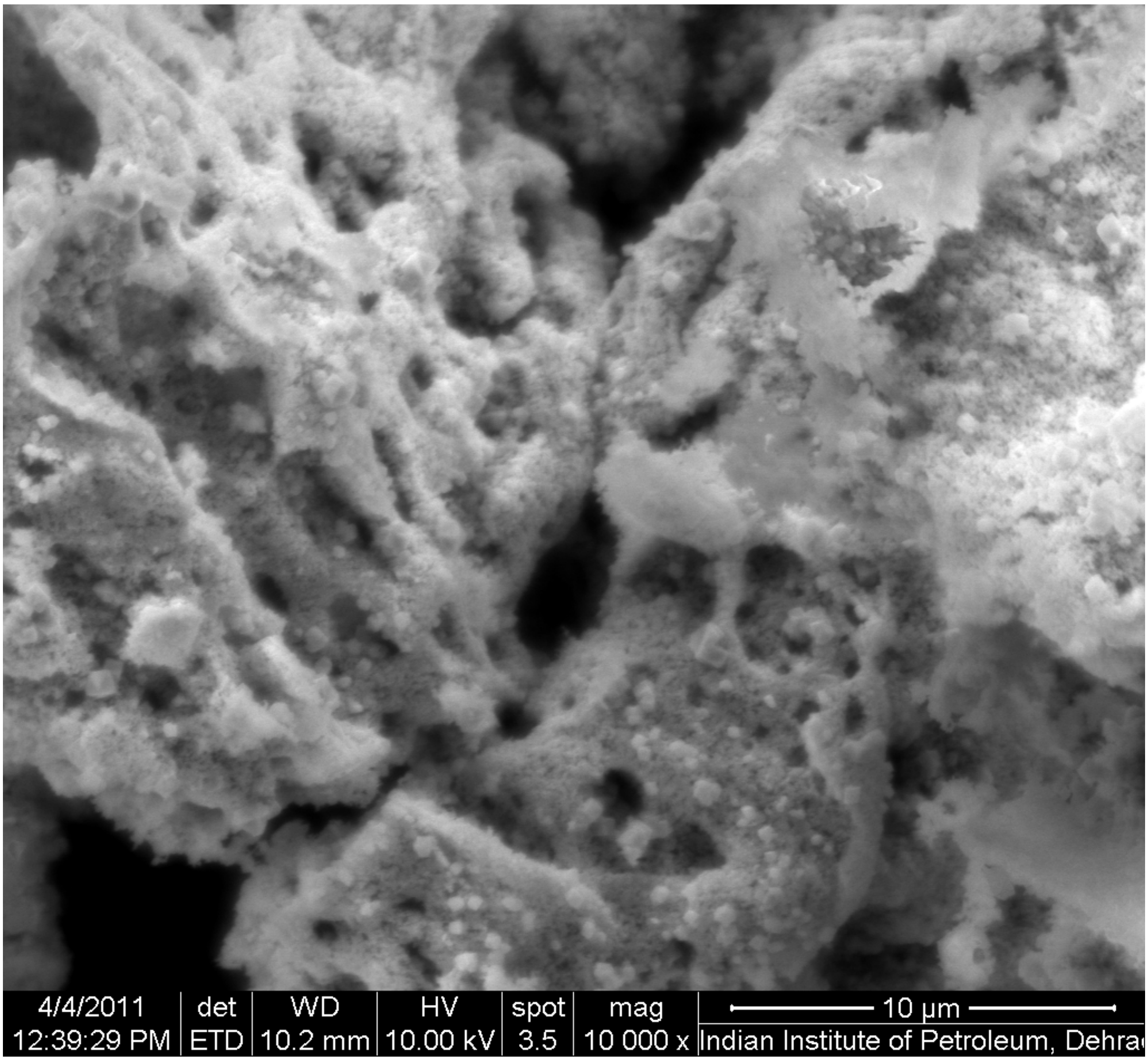

Fig. S5 SEM image of Cu-Cr catalyst without using cetyl alcohol.

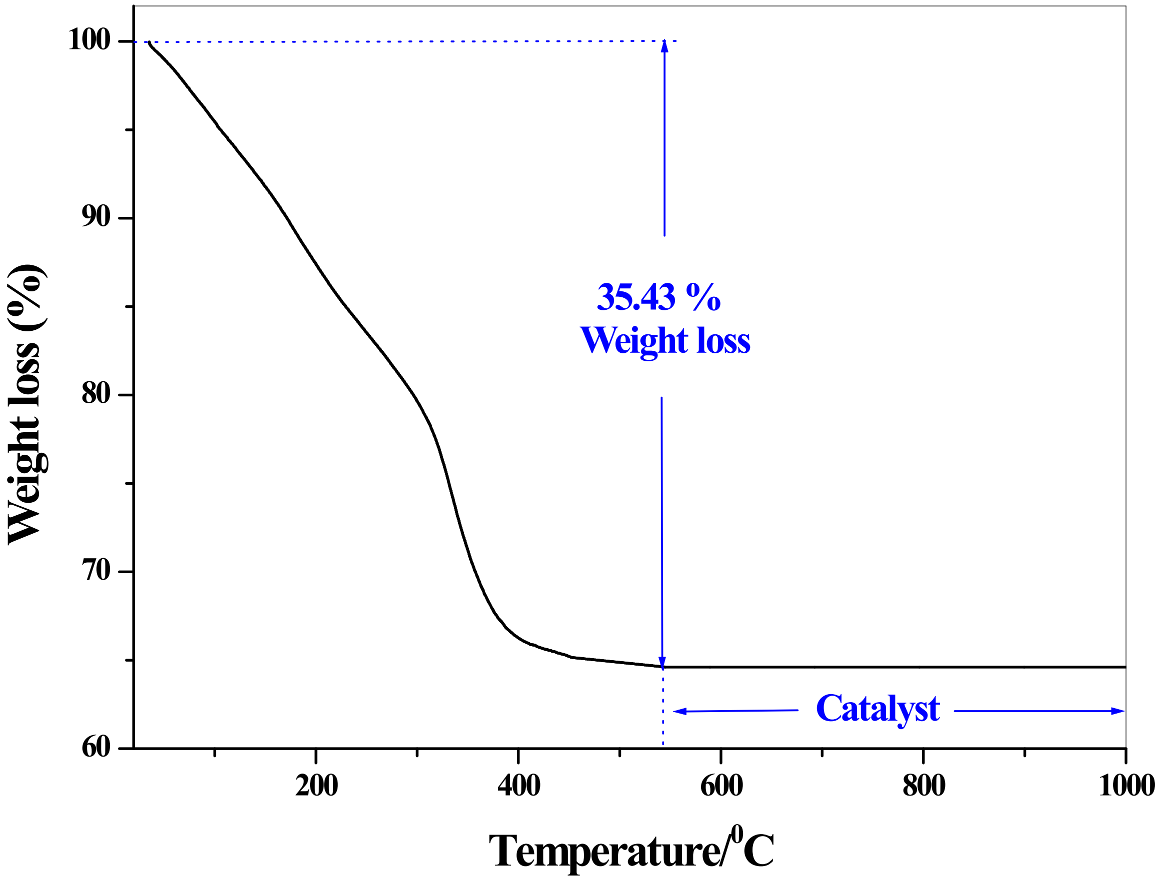

Fig. S6 TGA of the uncalcined $CuCr_2O_4$ spinel nanoparticles

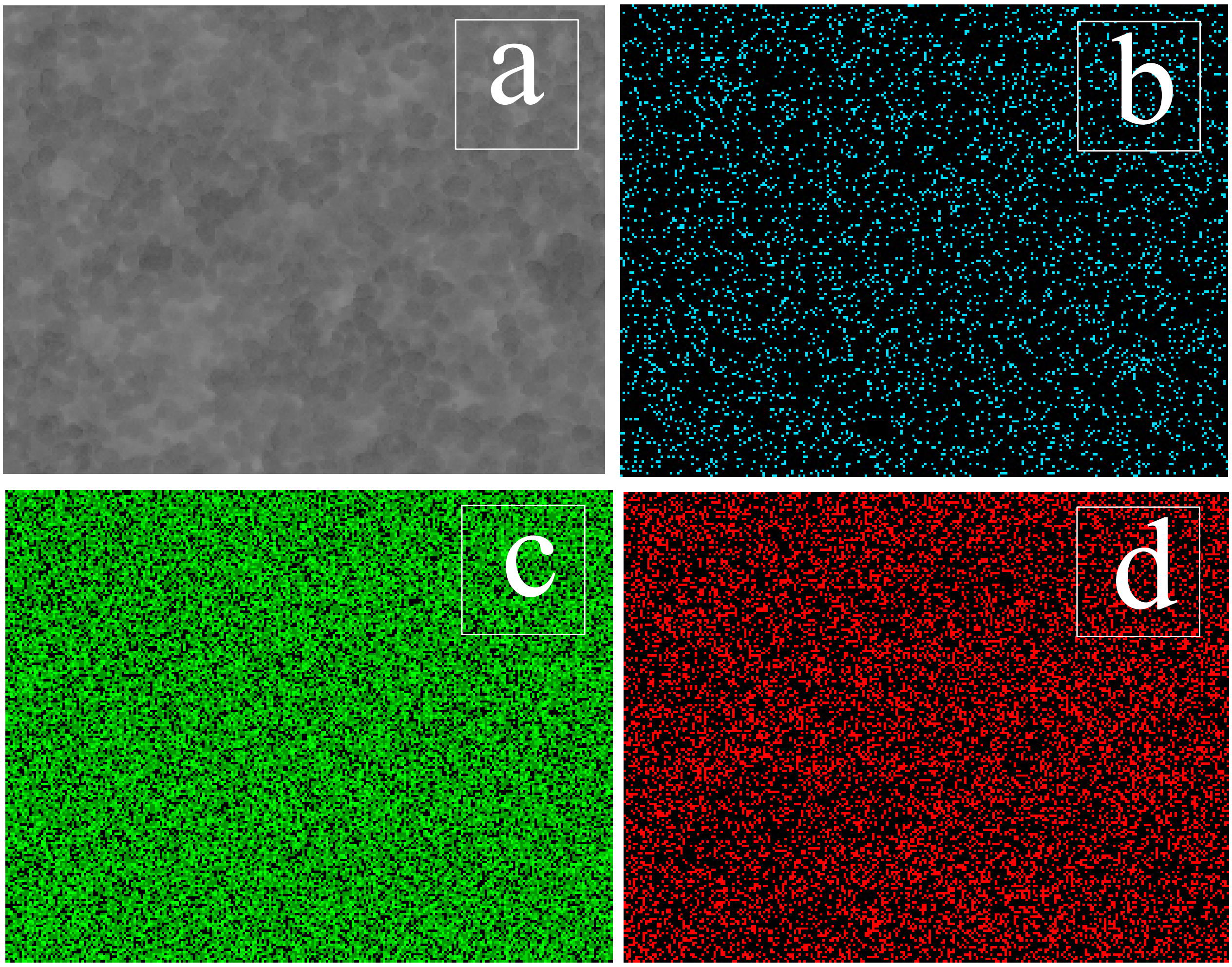

Fig. S7 Elemental mapping (b-d) for each element (Cu, Cr and O respectively) of $CuCr_2O_4$ spinel nanoparticles catalyst (based on Fig.2 a, main manuscript)

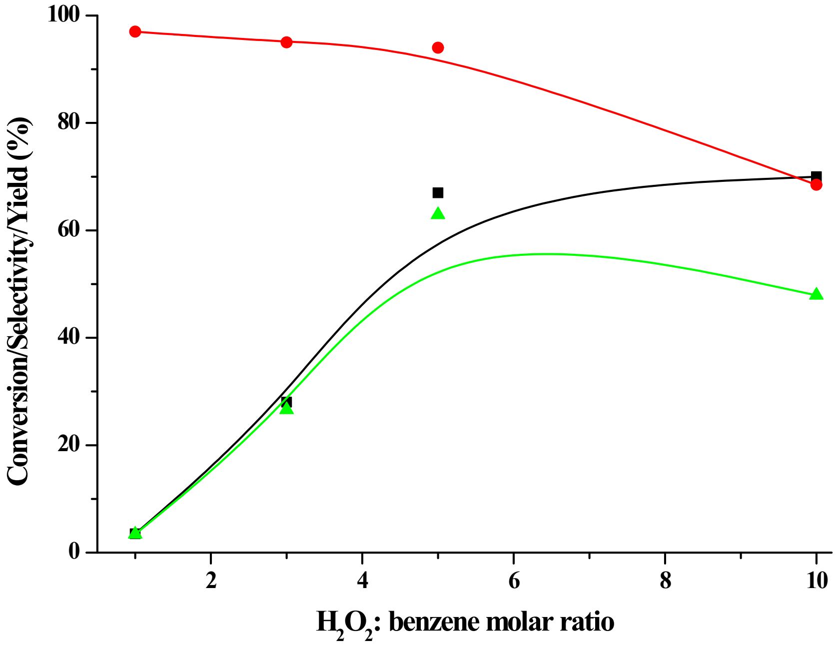

Fig. S8 Effect of H_2O_2: benzene molar ratio on benzene hydroxylation.

[■] Conversion of benzene; [●] Selectivity to phenol; [▲] Yield of phenol

Reaction Condition: benzene =1g; catalyst = 0.05g; temperature = 75 °C; time= 12 h.

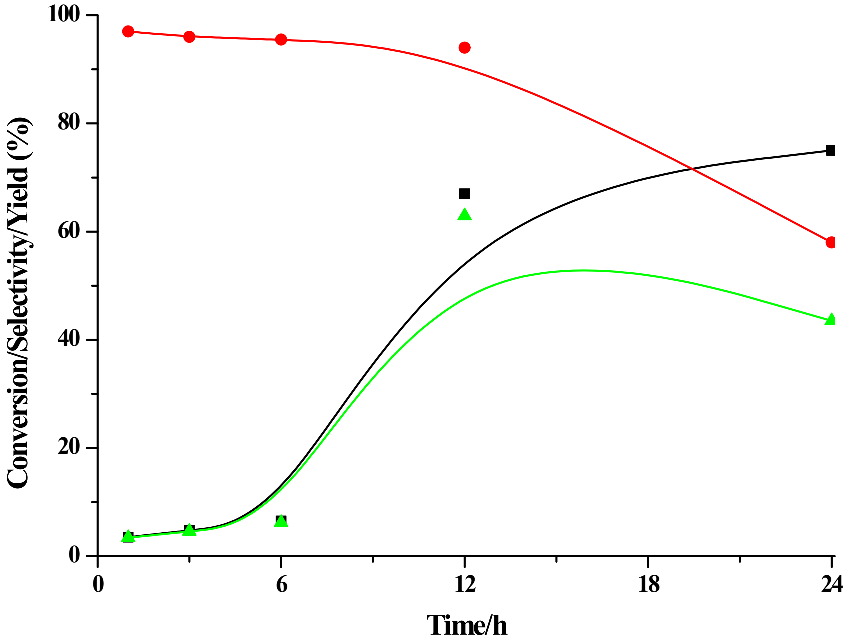

Fig. S9 Effect of time on benzene hydroxylation.

[■] Conversion of benzene; [●] Selectivity to phenol; [▲] Yield of phenol.

Reaction Condition: benzene =1g; benzene: H_2O_2 mole ratio =1:5; catalyst = 0.05g; temperature = 75 °C.

Table S1. Comaparative studies on benzene hydroxylations using various catalysts.

Entry	**Catalyst**	**Oxidant (Benzene: H_2O_2 Molar ratio)**	**Temp (°C)**	**Time (h)**	**C_B (%)**	**S_P (%)**	**Ref**
1	TS-1	H_2O_2 1:2.9	62°C	2	31	95	4
1	$FeSO_4.7H_2O$/AcOH	H_2O_2 1:0.1	50°C	1	8.4	97	5
2	Titanium silicate	H_2O_2 1:10	100°C	2	8.6	94	6
3	Methylimidiazolium-hexaflurophosphate	H_2O_2 1:1	50°C	6	54	71	7
4	$H_4PMo_{11}VO_{40}.13H_2O$	H_2O_2	RT		28.57	91	8
5	Clay-VO_x	H_2O_2 4:7	40°C	4	14	94	9
6	$PMoV_2$	H_2O_2 1:3	65°C	6	34.5	100	10
7	Tp*Cu(NCMe) Complexes	H_2O_2 1:1.5	80°C	2	21	81	11
8	V-Mesoporous organosilica	H_2O_2 1:3	50°C	8	27	100	12
9	A heteropolyanion-based cross-linked ionic copolymer (prepared by the anion-exchange of heteropolyacid $H_5PMo_{10}V_2O_{40}$ with polymeric ionic liquid poly(divinylbenzene-3-n-butyl-1vinylimidazolium)Br	H_2O_2 1:3	55°C	6	23.7	100	13
10	$[C_3CNpy]_4HPMoV_2$ (Phase-transfer)	H_2O_2 1:3	60 °C	2	87	95.8	14
11	C_3N_4-$H_5PMo_{10}V_2O_{40}$	O_2 2MPa in 50% AcOH-H_2O + Li OAc	130 °C	4.5	13.6	100	15
12	$CuCr_2O_4$ spinel nanoparticles (prepared by using cetyltrimethylammonium bromide)	H_2O_2 1:5	80 °C	12	72.5	94	16
13	**$CuCr_2O_4$ spinel nanoparticles (prepared by using cetyl alcohol)**	**H_2O_2 1:5**	**75 °C**	**12**	**67**	**94**	**This work**

References

1. F. Severino, J. Brito, O. Carfas and J. Laine, *J. Catal.,* 1986, **102**, 172.
2. F. Severino, J. L. Brito, J. Laine, J. L. G. Fierro and A. J. López Agudoy, *J. Catal.,* 1998, **177**, 82.
3. G. Pantaleo, L. F. Liotta, A. M. Venezia, G. Deganello, E. M. Ezzo, M. A. Kherbawi and H. Atia, *Mater. Chem. Phys.,* 2009, **114**, 604.
4. P. T. Tanev, M. Chibwe and T. J. Pinnavaia, *Nature,* 1994*,* **368**, 321.
5. D. Bianchi, R. Bortolo, R. Tassinari, M. Ricci and R. Vignola, *Angew. Chem.,* 2000, **39**, 4321.
6. L. Balducci, D. Bianchi, R. Bortolo, R. D'Aloisio, M. Ricci, R. Tassinari and R. Ungarelli, *Angew. Chem.,* 2003, **115,** 5087.
7. J. Peng, F. Shi, Y. Gu and Y. Deng, *Green Chem.* 2003, **5**, 224.
8. J. Zhang, T. Tang, G. Li and C. Hu, *Appl. Catal. A.,* 2005, **278**, 251.
9. X. Gao and J. Xu, *Appl. Clay Sci.,* 2006, **33**, 1.
10. F. Zhang, M. Guo, H. Ge and J. Wang, *Chin. J. Chem. Eng.,* 2007, **15**, 895.
11. A. Conde, Díaz-Requejo and P. Z. Pe′rez, *Chem. Commun.*, 2011, 8154.
12. P. Borah, X. Ma, K. T. Nguyen and Y. Zhao, *Angew. Chem.,* 2012, **51**, 7756.
13. P. Zhao, Y. Leng and J. Wang, *Chem. Eng. J.,* 2012, **204**, 72.
14. P. Zhao, J. Wang, G. Chen, Y. Zhou and J. Huang, *Catal. Sci. Technol*., 2013, **3**, 1394.
15. Z. Long, Y. Zhou, G. Chen, W. Ge and J. Wang, *Sci. Rep.,* 2014, **4**, 3651, DOI:10.1038/srep03651.
16. S. S. Acharyya, S. Ghosh, S. Adak, T. Sasaki and R. Bal. Catal. Sci. Technol. 2014, **4**, 4232.